ADVANCED MATERIALS
www.advmat.de

Self-heating and External Strain Coupling Induced Phase Transition of VO_2 Nanobeam as Single Domain Switch

Bin Hu, Yan Zhang, Wen Chen, Chen Xu, and Zhong Lin Wang**

VO_2, a strongly correlated oxide, displays a phase transition from insulator to metal (MIT) when heated it to its critical temperature (T_c) of 68 °C. The accompanied gigantic change in resis tivity and optical transmittance has attracted interest to explore the fundamental physical mechanism behind the transition.[1] Besides by temperature, this transition can also be driven by manipulation of various external stimuli, such as pressure, metal doping, photo-carrier injection and electric field, which have a profound effect on the phase transition. However, to date most works have been carried out based on epitaxial thin films or bulk crystals, in which the spatially inhomogeneous polycrystalline domains, local internal strain, and defects in the system result in the discontinuous and irregular phase domain structures when the transition occurs. If one takes the case of the temperature-induced transition process as an example, the system resistance decreases gradually over a wide temperature range, indicating the reordering of the introduced strain and secondary arrangement of phases within two- or three-dimensional structures. Therefore, it is difficult to realize independent control of temperature and strain, which may limit the application of VO_2 in novel devices.

Recently work by Cao *et al*. on one-dimensional VO_2 nanobeams brought the possibility to eliminate the irregular distribution of domains.[2] Single crystal, fine diameter and anisotropy with strain-sensitive growth direction (c_R, *c*-axis of rutile phase) make the formed metallic (M)/insulating (I) domain periodically aligning along the axis direction. Particularly, compared to the multiple-domain transition, the phase switch of a nanobeam based on a single domain has more potential applications in functional devices such as phase-change memories,[3] bolometric sensors,[4] and stationary Hadamard shutters,[5] all of which benefit from a much sharper change in electrical and optical properties. On the other hand, the one-dimensional geometry of the nanobeam can be easily loaded with external strain.[6] It is known that the MIT temperature (T_{MIT}) can be shifted up to 50 K by controlling the strain in VO_2 film through lattice mismatch growth, or by loading tensile or compressive external uniaxial stress in bulk VO_2.[7] The strain is also effective for the VO_2 nanobeam and more profound. Quantitative relationship between temperature and stress was built based on the uniaxial Clausius-Clapeyron equation and *M-I* phase diagram, thus, the coupled temperature-stain relationship can be utilized to understand the true behavior in VO_2.[8]

It has been demonstrated that single stimuli of ultrahigh compressive strain (2.2%) can drive the complete transition of a VO_2 nanobeam to the M phase at room temperature, and the critical loaded strain decreased with external heating. Nevertheless, an external heater is typically needed to achieve the T_{MIT}, which increases the complexity of the measurement system. Motivated by this challenge, in this report the external heating field was replaced by the simple Joule self-heating effect, which is caused by the dissipated power when the current runs through the nanobeam. This strategy has been used in metal oxide nanowires for low-power-cost thermistors[9] and gas sensors.[10] For these nanoscaled devices, a higher specific surface area and low-power consumption are responsible for the short thermal equilibrium time during the heat exchange. Here, by coupling the self-heating effect and external strain, we describe a new and simple way to fabricate a switch based on the single domain transition, which can maximum enhance the device sensitivity to a tiny strain, and this mechanical-electrical signal conversion with improved response performance brings the potential application of VO_2 nanobeam in strain monitor, and micro/nano-systems action control such as dynamic logic gate.[11]

High quality single-crystal VO_2 nanobeams were grown by a modified physical vapor deposition (PVD) following previous work.[12] Scanning electron microscopy (SEM) images in **Figures 1**a and b show the length of the nanobeam around several hundred micrometers with the growth direction along *a* axis of monoclinic insulating phase,[13] and the typical thickness and width are around 500 nm and 1 μm, respectively. The flexible and robust features of a VO_2 nanobeam make the manipulation easy using probes under optical microscope. A plastic plate was used as a substrate with the Kapton (HN) film covering on it (step 1 in Figure 1c), which can improve the thermal stability of the system owing to low thermal conductivity of Kapton (κ ~ 0.12 W/mK). The placed nanobeam was covered with mask and fixed by ~800 nm thickness Au/Cr electrodes at two ends using e-beam evaporation process, and the gap width is about 20 μm (Figure 1f). By this approach, the contact resistance decreased greatly compared to that using silver paste,[13] and the bendable real device is shown in Figure 1d.

One thing worth noting is a strain self-release process. In comparison to sputter deposition, the e-beam evaporation

B. Hu, Dr. Y. Zhang, C. Xu, Prof. Z. L. Wang
School of Materials Science and Engineering
Georgia Institute of Technology
Atlanta, GA 30332-0245, USA
E-mail: zhong.wang@mse.gatech.edu
B. Hu, Prof. W. Chen
State Key Laboratory of Advanced Technology for
Materials Synthesis and Processing
School of Materials Science and Engineering
Wuhan University of Technology
Wuhan, 430070, P. R. China
E-mail: chenw@whut.edu.cn

DOI: 10.1002/adma.201101731

© 2011 WILEY-VCH Verlag GmbH & Co. KGaA, Weinheim

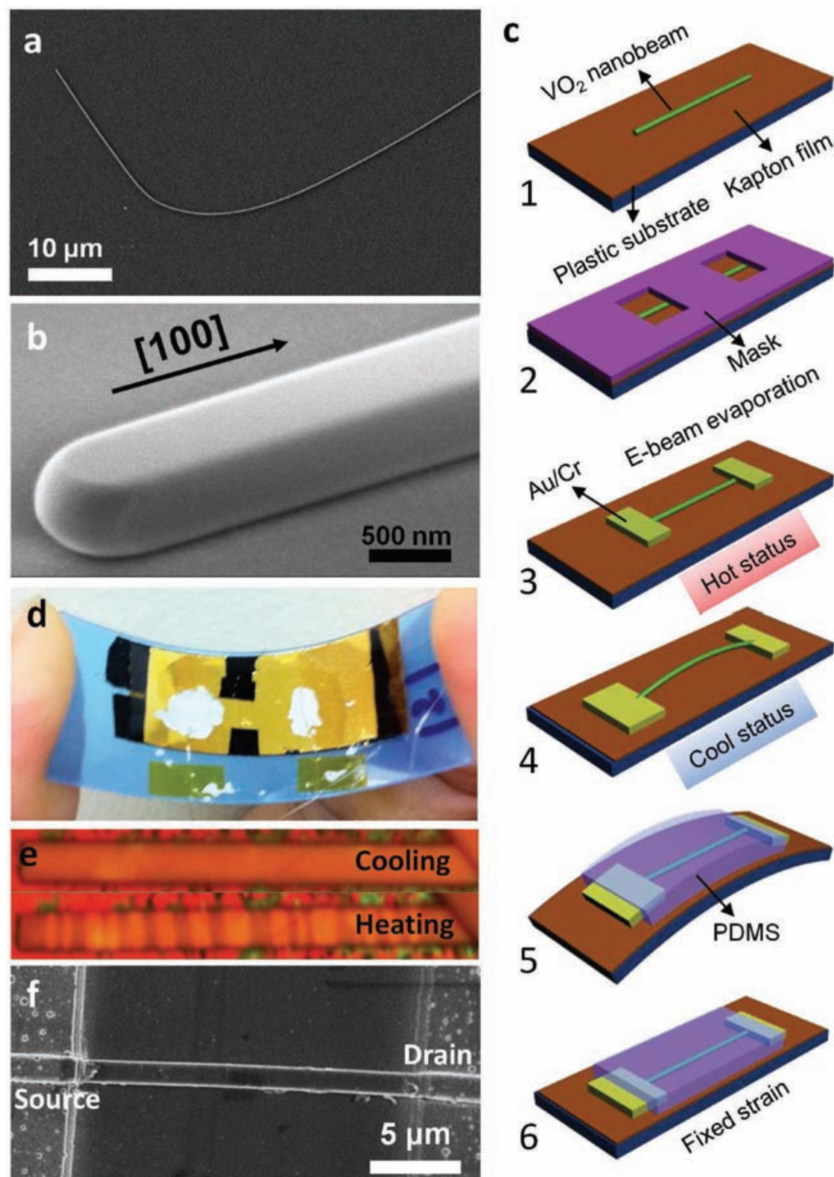

Figure 1. Structural characterization of VO_2 nanobeams and device fabrication. (a) SEM image of a flexible VO_2 nanobeam with (b) the detailed morphology of smooth surface, rectangular cross section and [100] growth direction. (c) E-beam evaporation was used for electrodes fabrication, and the nanobeam placed on Kapton was fixed by Au/Cr at two ends. Compressive strain created in the nanobeam after cooling down was released by self-arching, and further packaging by PDMS can fix the compression strain in the nanobeam. (d) Optical image of an as-fabricated device. (e) Optical images of a nanobeam that was fixed tightly on a SiO_2 substrate and the domain structure can be seen clearly after heating. (f) SEM image of a straight nanobeam after stretching the substrate as shown in step 5 of (c) and the gap width is about 20 μm.

method we used for device fabrication can provide relative high deposition temperature in the chamber (above 100 °C), which can drive the MIT of free-standing VO_2 nanobeam laid on the Kapton substrate, and accompanied by a structural phase transition (SPT) from a monoclinic structure to a tetragonal structure.[14] In another word, the nanobeam shrunk ~1.1% along the axis direction (c_R) during the depositing process. If the bottom side of the VO_2 nanobeam was firmly clamped on a substrate like SiO_2 during PVD synthesis process, after heating up to T_c the strain comes from the SPT and elastic mismatch across the interface will result in the self-organization of multiple M/I domains in the nanobeam (Figure 1e). For releasing the strain, Wei *et al*. used buffered oxide etch to remove the 1-μm-thick SiO_2 layer and suspended the nanobeam.[15] Similar but easier in our experiment, the end-fixed nanobeam has flexible free body which can get rid of the strain by self-arching without degrade or fracture (step 4 in Figure 1c). The strain-free body can switch between I and M phase with SPT crossed over the T_c by Joule-heating which will discuss in the following section (see Supplementary Information).

The original $I–V$ sweep characteristic was studied and in situ phase transition behavior was observed by optical microscopy. The upward bending of the $I–V$ curve with an applied voltage was due to the increased mobility of carriers in a semiconductor owing to Joule-heating (**Figure 2**a). Further increase the bias voltage up to 10.2 V caused an abrupt jump of current to 5 μA (compliance current), and the threshold resistivity (ρ_{th}) corresponding to the phase transition point is 9.8 Ω·cm.[16] The value of ρ_{th} was reported as a constant by Wei *et al*. (12 ± 2 Ω·cm)and Cao *et al*. (7 ± 2 Ω·cm).[2,15] However, ρ_{th} obtained here is between these two values, considering the different coefficients of thermal expansion for the substrate used in experiments, this is probably due to the different strain residual in the nanobeam after device fabrication (Kapton ~20 ppm/°C, SiO_2 ~0.5 ppm/°C, PC ~65–70 ppm/°C).[17] The inserted optical image in Figure 2a shows a notable change of reflection characteristic of the nanobeam from bright I phase to dark phase. Hole-driven MIT theory developed by Kim demonstrated that the Mott MIT occurs when the valence band is doped with hole charges of a very low critical density, and probably the change of carrier type from holes to electrons is responsible to this reflectivity change.[18]

There is a debate if the MIT is triggered by field-induced direct injection of charge or Joule heating, and is thus induced via the SPT, this is a particular significant question to understand true physics mechanism behind Mott transition. Some reports demonstrated that the MIT was triggered by applying high electrical field in VO_2 film or nanodot without causing the SPT, which indicated the T_{MIT} can be much lower than the T_{SPT}.[19] In contrast, in our case the observed SPT accompanied with MIT implied that the switch was agitated through self-heating up to T_c since the T_{SPT} always maintained above T_c regardless of correlation effect.[20] As seen in the

© 2011 WILEY-VCH Verlag GmbH & Co. KGaA, Weinheim

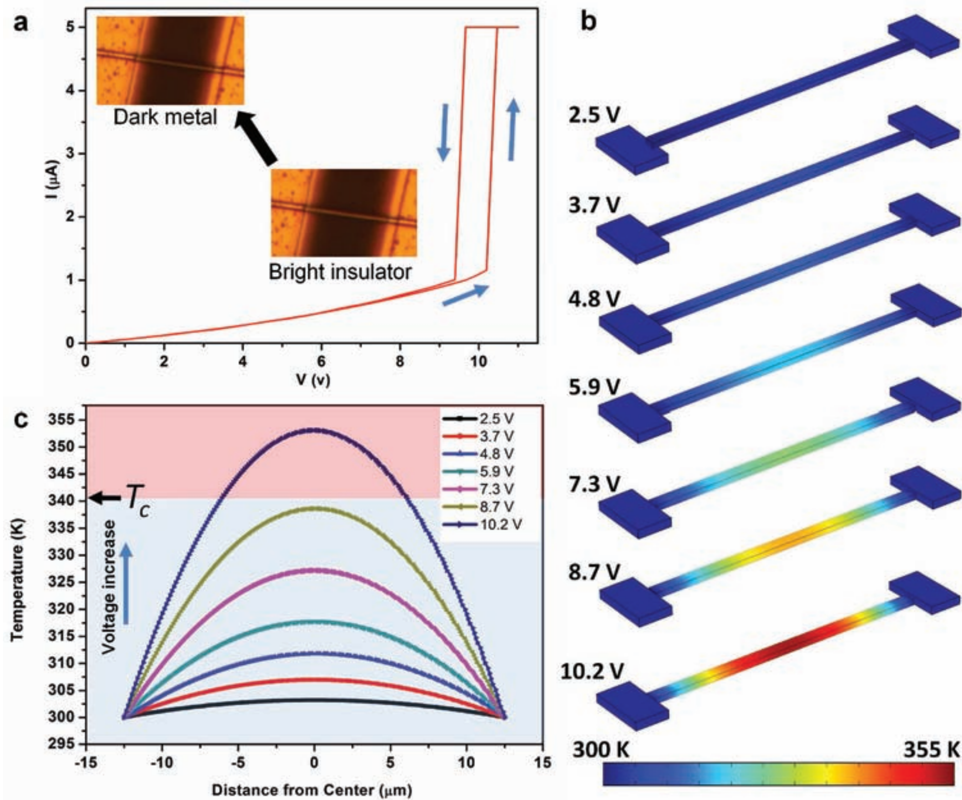

Figure 2. (a) Typical *I–V* curve of a bonded nanobeam that shows the MIT and pronounced hysteresis. Insets are optical images corresponding to the different status of bright I phase and dark M phase. (b) Finite element simulation of a VO_2 nanobeam with different voltages, the color map is a plot of the temperature of the surface, the blue color is room temperature and the dark red is 355 K. (c) Temperature line scan of a nanobeam with several values of bias voltages.

supporting video, the arched nanobeam (step 4 in Figure 1c) shrunk accompanying the current jump, and recovered after the current was off. The optical microcopy recorded the bent part from out-of-focus to in-focus, which strongly implies the SPT occurred in the device driven by Joule heating to T_c. Some electro-thermal simulations demonstrate that the Joule self-heating is insufficient to trigger the transition by itself when the electric field across the VO_2 thin film, and a typical temperature rise is less than 10 K.[21] Nevertheless, in this single crystal nanobeam system, observed SPT provides a good evidence that it is possible to reach the T_c by Joule self-heating. Moreover, no SPT and MIT were observed by applying pulse voltage (1 ms) at a magnitude of 10.2 V, indicating the heat accumulation was necessary for triggering SPT and the current switch was not due to the carrier increase casued by applied electrical field.

Simulations were carried out by modeling resistive heating using COMSOL Multiphysics software. The typical parameters of VO_2 nanobeam are 25 μm in length, 500 nm in thickness and 1 μm in width (Figure 1b) and ρ_{th} 9.8 $\Omega\cdot$cm. The contact resistance can be neglected and also the radiative heat loss because the computed temperature change is smaller than 50 K. The temperatures at the sides in contacting to the electrodes are initially set to 300 K. The gold pads are much larger than the width of the nanobeam with 800 nm in thickness and has much higher thermal conductivity compared to the surrounding medium and Kapton substrate, thus, its temperature is fixed at 300 K, while all other exterior surfaces are set as thermally insulating. Electro-thermal process in the nanobeam was simulated by the Fourier heat equation, with $\kappa = 2.5$W/mK, C_p = 690 J/kg·K, ρ = 4340 kg/m^3 being the thermal conductivity, specific heat, and mass density of VO_2, respectively. The various simulation voltages we chose here are corresponding to the critical voltage in the following electromechanical measurement. Figure 2b shows a simulated steady state temperature distribution in nanobeam. While the applied bias voltage is as low as 2.5 V, the self-heating in the nanobeam appears to be quite uniform, and corresponding temperature line scan along the nanobeam in Figure 2c shows only several degrees enhancement. With an increase in the voltage, the nanobeam was heated gradually, and as we observed in the experiment, the 10.2 V provides a high power that can break the T_c to simultaneously trigger the MIT and SPT. This local heating effect to drive the SPT by voltage was also reported in the study of the VO_2 memristor.[22] Since the actual temperature in the nanobeam can be complicated, which was probably lower than the simulation temperature because the simulated 10.2 V is overheated not just reach the T_c, and observed single domain indicated more uniform temperature distribution in the nanobeam. Therefore, a more precise model can be built by taking into account the electrodes heating and heat transfer with surrounding in the

© 2011 WILEY-VCH Verlag GmbH & Co. KGaA, Weinheim

further research. However, it offers the possibility of self-heating to T_{SPT}, and builds a qualitative relationship between the applied voltage and the raised temperature. In additional, a typical pronounced hysteresis of the *I–V* curve was observed in Figure 2a when the voltage scan was reversed, which exhibits similar behavior of temperature dependence of the resistivity,[23] and such a decreased T_{SPT} is due to the residual heating effect from the high temperature raised after transition.[24]

Besides the temperature-controlled transition, strain as an additional external stimulus can be introduced into the nanobeam by bending the substrate since the mechanical behavior of the entire structure is determined by the substrate. Firstly, a thin layer of polydimethylsiloxane (PDMS) was used to package the device to insure proper strain loading along the axis of the nanobeam in the following electromechanical measurement, and which can also improve the system stability. It needs to be mentioned that, for straightening the arched nanobeam laid on the substrate, the device was bent (Figure 1f) or heated up to T_{SPT} before packaging, and after fully polymerization of PDMS, compressive strain was fixed in the nanobeam (step 6 in Figure 1c). The fixed strain orginates both from spontaneous SPT and thermal expansion mismatch with the substrate. Considering the comparable coefficient of thermal expansion of Kapton and VO_2 at the device fabrication temperature,[25] the latter one can be negligible, i.e., only the SPT-induced compressive strain ~1.1% was frozen, which is a crucial point for a single domain switch.

The preloaded compressive strain results in a notable decrease of the MIT threshold voltage (V_{th}) to 8.7 V, and the fact that the corresponding ρ_{th} decreased to 8 Ω·cm implied that the compressive strain was maintained in the beam, which is consistent with previous reports.[15,17] The compressive strain dependence of the *I–V* curves for the device is shown in **Figure 3**a, and the V_{th} can be adjusted by modifying the uniaxial strain. The Saint-Venant bending theory is used to describe the linear relationship between maximum deflection of the substrate and the strain loaded on the nanobeam.[6a,26] With increasing external compressive strain, the V_{th} decreased step by step, as well as the threshold current, and ρ_{th} is a constant as we expected.[17] All of the currents abruptly jumped to 10 μA in compliance current and the lowest V_{th} we obtained can be decreased to 2.3 V with 0.93% external compressive strain, in which the total loaded strain was as high as ~2.03% plus the preloaded 1.1% strain, and corresponding T_{MIT} decreased to close to room temperature according to the simulation in Figure 2c. This critical strain value is very close to that obtained in pure-strain-induced room-temperature MIT.[2] For establishing a quantitative relationship between loaded strain and V_{th}, the strain–V_{th} curve of several typical devices is plotted in Figure 3b, although the V_{th} of non-bending devices are different because of many influencing factors during fabrication, all the curves have the similar variation tendency, which exhibits a linear relationship in the low strain region, while the V_{th} is more sensitive to the strain in the high compressive strain range.

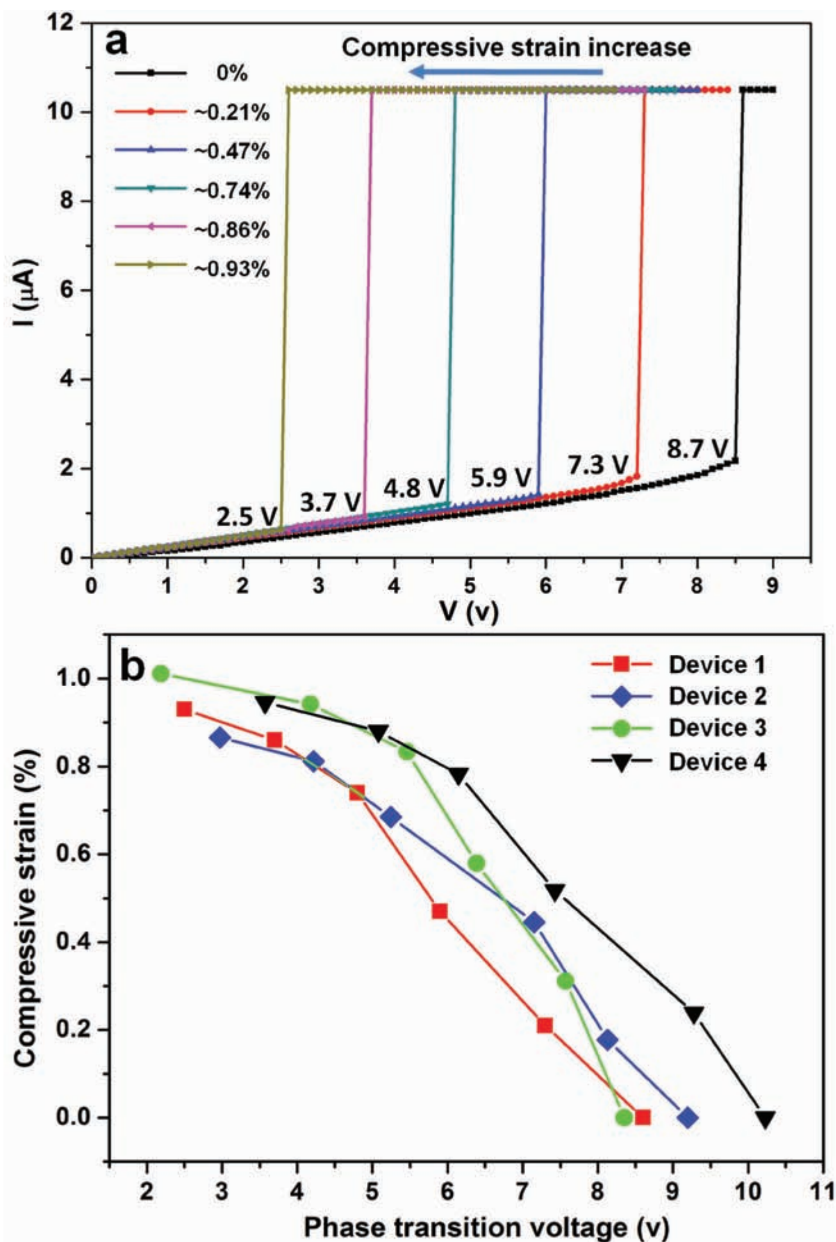

Figure 3. (a) *I–V* characteristic of packaged VO_2 nanobeam under different axial compressive strain, which shows that the threshold voltage and current decreased gradually with increasing the external compression. (b) Quantitative relationship between loaded strain and V_{th}.

Strain-induced T_c shift showed only 25% resistance change of MIT in the VO_2 film under low-frequency dynamic strain,[7d] and the lower resistance state was probably persisted even after

© 2011 WILEY-VCH Verlag GmbH & Co. KGaA, Weinheim

cooling down,[22] these are due to the inhomogeneous strain distribution and percolative nature of different phases. As a comparison, the VO_2 nanobeam exhibits a gigantic change of resistance up to several orders of magnitude by bending the substrate, which benefits from the single domain transition. As shown in **Figure 4**, the switch function of the device by coupling strain and self-heating effect is demonstrated. A series resistor of 5.4 kΩ was inserted in the circuit to avoid destruction of the nanobeam at the transition point. Firstly, for the M→I transition mode, a high DC voltage of 9.5 V was applied, which is sufficient high to induce the MIT in the nanobeam as shown in Figure 4a, and the current kept ~1.6 mA corresponded to ~5.7 kΩ resistance in the whole system. The comparable value to the series resistor indicated the fully transition of the nanobeam to the M phase, and the preloaded-compressive strain frozen in nanobeam can be released completely without formation of the tensile strain or spontaneous I domains, which is different from the sample grown on SiO_2.[15] When the substrate was stretched, the current abrupt dropped to ~2.4 μA, implying the reversed switch from M to I phase. The stretch decrease the preloaded compressive strain thus increase the V_{th} of MIT, and 9.5 V bias voltage is not high enough to maintain the nanobeam in M status, if the series resistor is not taken into account, the giant resistance change of the nanobeam can be as high as 4 orders of magnitude. Moreover, this switch is repeatable without decay by alternate stretch and release.

In contrast, but still explainable by the same mechanism, a further increase of the compressive strain in the nanobeam can trigger a transition, which cannot occur in the non-bent device. For the I→M transition mode as shown in Figure 4b, the bias voltage of 8 V was applied in the same device for preheating the nanobeam, and the current jumped from ~1.8 μA to ~1.4 mA after compressing the substrate, and it is repeatable as well. It needs to be mentioned that the compressive strain we employed is ~0.05%, which is much lower than the critical compressive for triggering the MIT without Joule-heating (higher than ~0.93% according Figure 3a); even when applying a low bias voltage (3 V), this tiny compressive strain cannot trigger the MIT either. Therefore, the effect from pure-strain-induced MIT can be ruled out. The typical switch time is shown in Figure 4c, which is the enlarged part of the dotted frame in Figure 4b. Considering the limitations of the electronic response of the measurement system, the response speed for current jump and drop can be faster than 0.15 s. A previous report on the X-ray study of the SPT showed that the response time can be as short as 1 ps,[27] and Hormoz *et al*. predicted the lower bound switching time to be on the order of 0.5 ps.[28] Therefore, this strain-controlled switch has a much higher sensitivity and control efficiency compared to that of bulk crystals and the film.

In summary, by coupling self-heating and external strain we offer a new way to tune the MIT in a single domain in order to improve VO_2-based device applications. By applying a bias voltage that exceeds V_{th}, the nanobeam can be self-heated to the M phase with SPT, and external strain can be utilized to modulate V_{th} precisely. M and I phases at two sides of V_{th} can be easily switched based on single domain transition by stretching or compressing the substrate, and the device exhibits great controllability with very efficient and quick switching. These features were demonstrated in this paper and can enable strategies for the integration of a VO_2 nanobeam in advanced and complex functional units such as logic gates for micro/nano-systems action control.

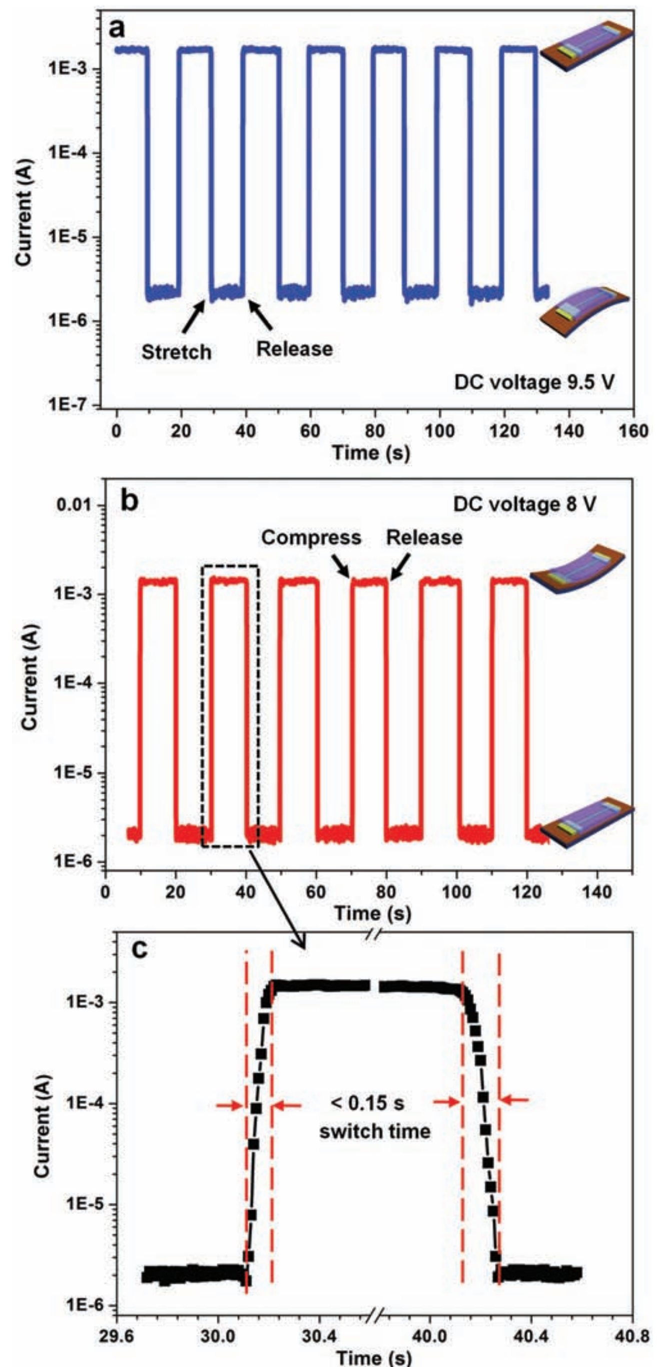

Figure 4. Electrical switch with the strain change based on single domain. (a) High DC voltage of 9.5 V applied on the device can trigger the MIT and kept the nanobeam in a low resistance status, which can be switched to a high resistance status by stretching the substrate. (b) Relative low DC voltage of 8 V applied on device driven the nanobeam close to the MIT, which can be triggered by compressing the substrate, and both switch in (a) and (b) are repeatable and stable. (c) The enlarged Figure of dotted frame in (b) shows the switch speed is fast than 0.15 s.

© 2011 WILEY-VCH Verlag GmbH & Co. KGaA, Weinheim

Supporting Information

Supporting Information is available from the Wiley Online Library or from the author.

Acknowledgements

This work was supported by DARPA, DOE BES, the NSFC (No: 51072152), the Fundamental Research Funds for the Central Universities of China (2010-VI-008) and Excellent Doctoral Thesis Project of WUT (2010-YB-03). B.H. thanks the China Scholarship Council for support and thanks Prof. L. Q. Mai for helpful discussion.

Received: May 9, 2011
Published online:

[1] a) M. M. Qazilbash, M. Brehm, G. O. Andreev, A. Frenzel, P. C. Ho, B.-G. Chae, B.-J. Kim, S. J. Yun, H.-T. Kim, A. V. Balatsky, O. G. Shpyrko, M. B. Maple, F. Keilmann, D. N. Basov, *Phys. Rev. B* **2009**, *79*, 075107; b) B. Lazarovits, K. Kim, K. Haule, G. Kotliar, *Phys. Rev. B* **2010**, *81*, 115117; c) A. C. Jones, S. Berweger, J. Wei, D. Cobden, M. B. Raschke, *Nano Lett.* **2010**, *10*, 1574; d) E. U. Donev, R. Lopez, L. C. Feldman, R. F. Haglund, *Nano Lett.* **2009**, *9*, 702.

[2] J. Cao, E. Ertekin, V. Srinivasan, W. Fan, S. Huang, H. Zheng, J. W. L. Yim, D. R. Khanal, D. F. Ogletree, J. C. Grossmanan, J. Wu, *Nat. Nanotechnol.* **2009**, *4*, 732.

[3] S. Meister, D. T. Schoen, M. A. Topinka, A. M. Minor, Y. Cui, *Nano Lett.* **2008**, *8*, 4562.

[4] M. Gurvitch, S. Luryi, A. Polyakov, A. Shabalov, *IEEE Trans. Nanotechnol.* **2010**, *9*, 647.

[5] M. Soltani, M. Chaker, E. Haddad, R. Kruzelecky, J. Margot, P. Laou, S. Paradis, *J. Vac. Sci. Technol. A* **2008**, *26*, 763.

[6] a) J. Zhou, Y. D. Gu, P. Fei, W. J. Mai, Y. F. Gao, R. S. Yang, G. Bao, Z. L. Wang, *Nano Lett.* **2008**, *8*, 3035; b) R. S. Yang, Y. Qin, L. M. Dai, Z. L. Wang, *Nat. Nanotechnol.* **2009**, *4*, 34.

[7] a) J. P. Pouget, H. Launois, J. P. Dhaenens, P. Merenda, T. M. Rice, *Phys. Rev. Lett.* **1975**, *35*, 873; b) P. Jin, K. Yoshimura, S. Tanemura, *J. Vac. Sci. Technol. A* **1997**, *15*, 1113; c) Y. Muraoka, Y. Ueda, Z. Hiroi, *J. Phys. Chem. Solids* **2002**, *63*, 965-967; d) T. Kikuzuki, M. Lippmaa, *Appl. Phys. Lett.* **2010**, *96*, 132107.

[8] a) J. Cao, Y. Gu, W. Fan, L. Q. Chen, D. F. Ogletree, K. Chen, N. Tamura, M. Kunz, C. Barrett, J. Seidel, J. Wu, *Nano Lett.* **2010**; b) W. Fan, S. Huang, J. Cao, E. Ertekin, C. Barrett, D. R. Khanal, J. C. Grossman, J. Wu, *Phys. Rev. B* **2009**, *80*, 241105.

[9] E. Strelcov, Y. Lilach, A. Kolmakov, *Nano Lett.* **2009**, *9*, 2322.

[10] a) E. Strelcov, S. Dmitriev, B. Button, J. Cothren, V. Sysoev, A. Kolmakov, *Nanotechnology* **2008**, *19*; b) J. D. Prades, R. Jimenez-Diaz, F. Hernandez-Ramirez, S. Barth, A. Cirera, A. Romano-Rodriguez, S. Mathur, J. R. Morante, *Appl. Phys. Lett.* **2008**, *93*; c) B. Hu, L. Q. Mai, W. Chen, F. Yang, *ACS Nano* **2009**, *3*, 478; d) L. Mai, L. Xu, Q. Gao, C. Han, B. Hu, Y. Pi, *Nano Lett.* **2010**, *10*, 2604.

[11] W. Wu, Y. Wei, Z. L. Wang, *Adv. Mater.* **2010**, *22*, 4711.

[12] B. S. Guiton, Q. Gu, A. L. Prieto, M. S. Gudiksen, H. Park, *J. Am. Chem. Soc.* **2005**, *127*, 498.

[13] B. Hu, Y. Ding, W. Chen, D. Kulkarni, Y. Shen, V. V. Tsukruk, Z. L. Wang, *Adv. Mater.* **2010**, *22*, 5134.

[14] F. J. Morin, *Phys. Rev. Lett.* **1959**, *3*, 34.

[15] J. Wei, Z. H. Wang, W. Chen, D. H. Cobden, *Nat. Nanotechnol.* **2009**, *4*, 420.

[16] The length of the nanobeam is about 45 μm in operated device which is longer than the gap. This is because of the tear of the connection between nanobeam and deposited Au/Cr electrodes, which is caused by the expansion of the nanobeam along the axis direction after device cooling down.

[17] J. Cao, W. Fan, K. Chen, N. Tamura, M. Kunz, V. Eyert, J. Wu, *Phys. Rev. B* **2010**, *82*, 241101.

[18] a) H. T. Kim, B. G. Chae, D. H. Youn, S. L. Maeng, G. Kim, K. Y. Kang, Y. S. Lim, *New J. Phys.* **2004**, *6*; b) H.-T. Kim, B.-J. Kim, Y. W. Lee, B.-G. Chae, S. J. Yun, *Phys. B: Conden. Matter* **2008**, *403*, 1434.

[19] a) K. Okimura, N. Ezreena, Y. Sasakawa, J. Sakai, *Jpn. J. Appl. Phys.* **2009**, *48*; b) D. Ruzmetov, G. Gopalakrishnan, J. Deng, V. Narayanamurti, S. Ramanathan, *J. Appl. Phys.* **2009**, *106*, 083702; c) J. S. Lee, M. Ortolani, U. Schade, Y. J. Chang, T. W. Noh, *Appl. Phys. Lett.* **2007**, *91*, 133509.

[20] H.-T. Kim, Y. W. Lee, B.-J. Kim, B.-G. Chae, S. J. Yun, K.-Y. Kang, K.-J. Han, K.-J. Yee, Y.-S. Lim, *Phys. Rev. Lett.* **2006**, *97*, 266401.

[21] G. Gopalakrishnan, D. Ruzmetov, S. Ramanathan, *J. Mater. Sci.* **2009**, *44*, 5345.

[22] T. Driscoll, H.-T. Kim, B.-G. Chae, M. D. Ventra, D. N. Basov, *Appl. Phys. Lett.* **2009**, *95*, 043503.

[23] L. Q. Mai, B. Hu, T. Hu, W. Chen, E. D. Gu, *J. Phys. Chem. B* **2006**, *110*, 19083.

[24] D.-W. Oh, C. Ko, S. Ramanathan, D. G. Cahill, *Appl. Phys. Lett.* **2010**, *96*, 151906.

[25] D. Kucharczyk, T. Niklewski, *J. Appl. Crystallogr.* **1979**, *12*, 370.

[26] R. W. Soutas-Little, in *Elasticity*, Vol. *XVI*, Dover Publications, Mineola, NY**1973**, p. 431.

[27] A. Cavalleri, C. Tóth, C. W. Siders, J. A. Squier, F. Ráksi, P. Forget, J. C. Kieffer, *Phys. Rev. Lett.* **2001**, *87*, 237401.

[28] S. Hormoz, S. Ramanathan, *Solid-State Electronics* **2010**, *54*, 654.

© 2011 WILEY-VCH Verlag GmbH & Co. KGaA, Weinheim